Moving Adaptive Grids (part 4)

P. A. Zegeling

Mathematical Institute
The Netherlands

Universiteit Utrecht

Winterschool
December 1-2, 2018, Moscow

Contents of part 4

Parameter-free non-singular moving grids in 2D:

- Theory & properties
- Application to a tumour model
- Application to resistive Magneto-hydrodynamics
- Application to the 2D Euler equations
- Extension to 3D and application to blow-up models

Physical vs. computational coordinates [1]

The 2D adaptive grid can also be seen as an approximation of a coordinate transformation between computational coordinates

$$(\xi, \eta)^T \in \Omega_c := [0, 1] \times [0, 1]$$

(with a uniform grid partitioning) and physical coordinates

$$(x, y)^T \in \Omega_p \subset \mathbb{R}^2$$

(with a non-uniform adaptive grid)

Physical vs. computational coordinates [2]

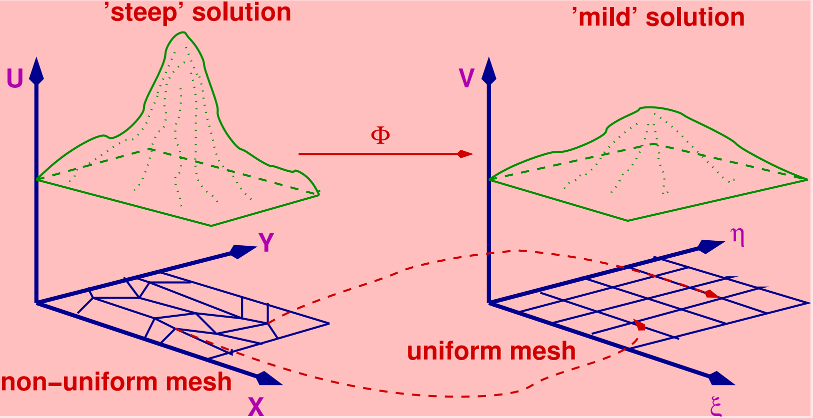

Winslow's method

In a variational setting, a 'grid-energy' functional (à la Winslow) can be defined as

$$\mathcal{E} = \frac{1}{2} \iint_{\Omega_c} \left(\nabla^T x \, \omega \, \nabla x + \nabla^T y \, \omega \, \nabla y \right) \; d\xi d\eta,$$

where $\nabla = (\frac{\partial}{\partial \xi}, \frac{\partial}{\partial \eta})^T$ and $\omega > 0$ is a monitor function.
Minimizing the energy $\mathcal{E}$ yields the Euler-Lagrange equations:

$$\boxed{\begin{aligned} \nabla \cdot (\omega \nabla x) = 0 \\ \nabla \cdot (\omega \nabla y) = 0 \end{aligned}}$$

on $\Omega_c = [0,1] \times [0,1]$ with BCs:

$x|_{\xi=0} = x_L, \;\; y|_{\eta=0} = y_L, \;\; x|_{\xi=1} = x_R, \;\; y|_{\eta=1} = y_U,$
$\frac{\partial x}{\partial n}|_{\xi=0} = \frac{\partial x}{\partial n}|_{\xi=1} = \frac{\partial y}{\partial n}|_{\eta=0} = \frac{\partial y}{\partial n}|_{\eta=1} = 0.$

The adaptive grid seen as a system of springs

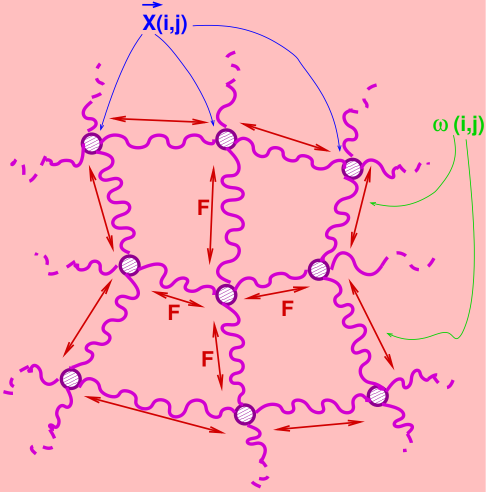

Regularity of the transformation in 2D

Theorem [Clément, Hagmeijer & Sweers, '96]:

Let $\omega \geq \tilde{c} > 0$, $\omega \in C^{0,1}(\Omega_c)$ *and* $\omega_\xi, \omega_\eta \in C^\gamma(\bar{\Omega}_c)$, *for some* $\gamma \in (0,1)$.
$\Rightarrow$ $\exists$ *unique solution* $(x, y) \in C^2(\bar{\Omega}_c)$, *which is a bijection from* $\bar{\Omega}_c$ *into itself. Moreover, the Jacobian satisfies:*

$$\mathcal{J} = x_\xi y_\eta - x_\eta y_\xi > 0.$$

The three main ingredients of proof are:

- Carleman-Hartman-Winter Theorem (3D??)
- Jordan Curve Theorem (3D??)
- Maximum principle for elliptic PDEs (3D ok!)

A few additional properties of the 2D grid

Equidistribution in 1D: $\underbrace{x_\xi}_{\mathcal{J}} \quad \omega = \text{cst}$

Winslow in 2D: $\nabla(x_\xi) \cdot \nabla(y_\eta) - \nabla(x_\eta) \cdot \nabla(y_\xi) = 0 \Rightarrow \mathcal{J} \; \omega = \text{cst}$

(remember: $\mathcal{J} = x_\xi y_\eta - x_\eta y_\xi$)

⋆ the transformation behind Winslow's method is *not* a harmonic mapping, but it is *related* to it

⋆ a counterexample can be given for the 3D (harmonic) case, for which the transformation looses its regularity (Liao et al '94)

⋆ several components in the proof of the 2D Theorem can *not* be applied in 3D either...

The monitor function ω

Arclength-type (AL-) monitor:

$$\omega = \sqrt{1 + \alpha \ \nabla u \cdot \nabla u}$$

α is a (problem-dependent) ‘adaptivity’-parameter which controls the amount of adaptivity.

BM-monitor (Beckett & Mackenzie $\geq$ ’01):

$$\omega = \alpha(t) + ||\nabla u||_2^{\frac{1}{m}}, \quad \text{with} \quad \alpha(t) = \iint_{\Omega_c} ||\nabla u||_2^{\frac{1}{m}} \ d\xi d\eta$$

$m = 1$: better scaling and more adaptivity than for $m = 2$

Smoothness of the BM monitor function

Define (Huang '02) $\bar{\omega} = 1 + \frac{\gamma ||\nabla u||_2}{(1-\gamma) \iint_{\Omega_c} ||\nabla u||_2 \; d\xi d\eta}$ with $\gamma \in [0, 1)$

$$\Rightarrow \gamma = \frac{\iint_{\Omega_c} \bar{\omega} \; d\xi d\eta \; - 1}{\iint_{\Omega_c} \bar{\omega} \; d\xi d\eta}$$

For $\gamma = \frac{1}{2}$, we have $\bar{\omega} = 1 + \frac{||\nabla u||_2}{\iint_{\Omega_c} ||\nabla u||_2 \; d\xi d\eta} \Rightarrow \approx$ 50% of the grid points is concentrated in regions of high spatial derivatives, since

- $\iint_{\Omega_c} \bar{\omega} \; d\xi d\eta \sim$ the total # of grid points
- $\iint_{\Omega_c} \bar{\omega} \; d\xi d\eta - 1 \sim$ the # of grid points in the steep layer

$\Longrightarrow$ a smoother distributed grid than for the AL-monitor (with constant α) and $\alpha(t)$ is automatically computed!

Smoothing of the AL-monitor function

With the BM-monitor, application of a filter or smoother to the grid or monitor values is not necessary.
Normally, smoother transitions in a general non-uniform grid can be obtained (and are needed!) by working with the smoothed value

$$\mathcal{S}(\omega_{i+\frac{1}{2},j+\frac{1}{2}}) = \frac{1}{4}\omega_{i+\frac{1}{2},j+\frac{1}{2}} + \frac{1}{8}(\omega_{i+\frac{3}{2},j+\frac{1}{2}} + \omega_{i-\frac{1}{2},j+\frac{1}{2}} + \omega_{i+\frac{1}{2},j+\frac{3}{2}}$$

$$+\omega_{i+\frac{1}{2},j-\frac{1}{2}}) + \frac{1}{16}(\omega_{i-\frac{1}{2},j-\frac{1}{2}} + \omega_{i-\frac{1}{2},j+\frac{3}{2}} + \omega_{i+\frac{3}{2},j-\frac{1}{2}} + \omega_{i+\frac{3}{2},j+\frac{3}{2}})$$

In the numerical experiments we denote this with *filter on* or *filter off* (working merely with $\omega_{i+\frac{1}{2},j+\frac{1}{2}}$ values i.e. $\mathcal{S}(\omega) = \omega$).

Application 1: a 2D tumour model [1]

M.A.J. Stuart & A.M. Stuart,
A model mechanism for the chemotactic response of endothelial cells to tumour angiogenesis factor,
IMA Journal of Mathematics, V10, 1993.

$$
\begin{aligned}
u_t &= \epsilon_1 \Delta u - \nabla \cdot (u\kappa \nabla u) + \mu u\,(1-u)\max\{0, v - v^*\} - \delta u \\
v_t &= \epsilon_2 \Delta v - \lambda v - \tfrac{\phi u v}{\gamma + v}
\end{aligned}
$$

Application 1: a 2D tumour model [2]

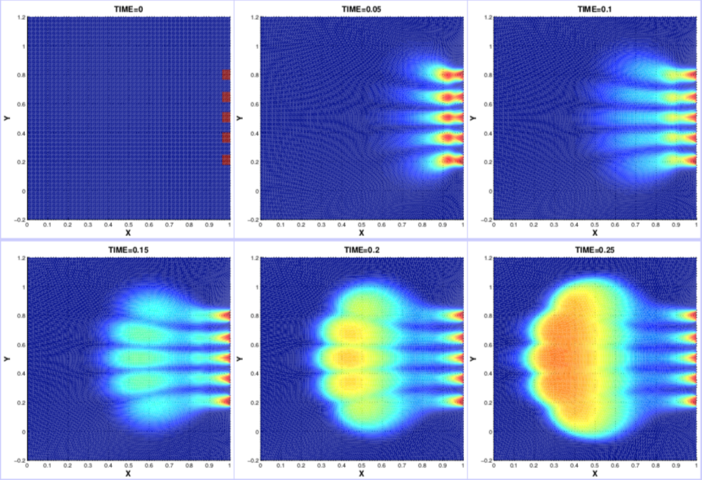

Application 1: a 2D tumour model [3]

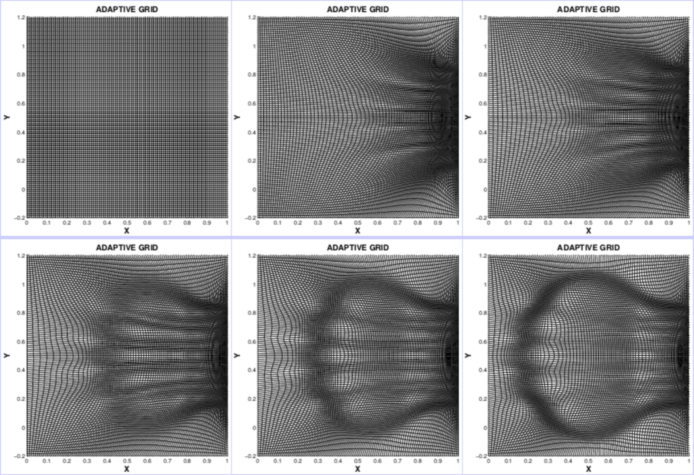

Application 2: resistive Magneto-HydroDynamics

$$\frac{\partial \rho}{\partial t} + \nabla \cdot (\rho \mathbf{v}) = 0$$

$$\frac{\partial (\rho \mathbf{v})}{\partial t} + \nabla \cdot (\rho \mathbf{v}\mathbf{v} - \mathbf{B}\mathbf{B}) + \nabla p_{tot} = 0$$

$$\frac{\partial e}{\partial t} + \nabla \cdot (\mathbf{v} e + \mathbf{v} p_{tot} - \mathbf{B}\mathbf{B} \cdot \mathbf{v}) = \eta_m (\nabla \times \mathbf{B})^2$$

$$\frac{\partial \mathbf{B}}{\partial t} + \nabla \cdot (\mathbf{v}\mathbf{B} - \mathbf{B}\mathbf{v}) = \eta_m \Delta \mathbf{B}$$

$$p_{tot} = p + \frac{\mathbf{B}^2}{2}, \quad p = (\gamma - 1)(e - \rho \frac{\mathbf{v}^2}{2} - \frac{\mathbf{B}^2}{2})$$

Where can we find these models?

Kinematic flux expulsion in 2D [1]

$$\frac{\|\mathbf{B}\|^2}{8\pi\mu} \ll \frac{1}{2}\rho\|\mathbf{v}\|^2 \Rightarrow$$

$$\frac{\partial \mathbf{B}}{\partial t} = \nabla \times (\mathbf{v} \times \mathbf{B}) + \eta_m \Delta \mathbf{B}$$

$$\text{with} \quad \nabla \cdot \mathbf{v} = 0$$

$$\frac{\partial}{\partial z} = 0,\ \mathbf{B} = (B_1, B_2, 0),\ \nabla \cdot \mathbf{B} = 0 \Rightarrow$$

$$\frac{\partial B_1}{\partial t} = \eta_m \Delta B_1 + v_1 \frac{\partial B_2}{\partial y} - v_2 \frac{\partial B_1}{\partial y} + B_2 \frac{\partial v_1}{\partial y} - B_1 \frac{\partial v_2}{\partial y}$$

$$\frac{\partial B_2}{\partial t} = \eta_m \Delta B_2 - v_1 \frac{\partial B_2}{\partial x} + v_2 \frac{\partial B_1}{\partial x} - B_2 \frac{\partial v_1}{\partial x} + B_1 \frac{\partial v_2}{\partial x}$$

Kinematic flux expulsion in 2D [2]

$$\mathbf{B} := \nabla \times \mathbf{A} \ , \quad \text{where } \mathbf{A} := \text{vector potential} \Rightarrow$$

$$\frac{\partial \mathbf{A}}{\partial t} = \mathbf{v} \times (\nabla \times \mathbf{A}) - \eta_m \nabla \times (\nabla \times \mathbf{A})$$

$$B_3 = 0 \ (\Rightarrow A_1 = A_2 \equiv 0) :$$

$$\frac{\partial A_3}{\partial t} = -v_1 \frac{\partial A_3}{\partial x} - v_2 \frac{\partial A_3}{\partial y} + \eta_m \Delta A_3$$

where $v_1(x, y)$ and $v_2(x, y)$ are given and satisfy

$$\frac{\partial v_1}{\partial x} + \frac{\partial v_2}{\partial y} = 0$$

Kinematic flux expulsion in 2D [3]

Four-cell convection (Weiss '66):

$$v_1(x,y) = \sin(2\pi x)\cos(2\pi y)$$
$$v_2(x,y) = -\cos(2\pi x)\sin(2\pi y)$$

$$0 < \eta_m \ll 1, \quad A_3|_{t=0} = 1 - x$$

$$A_3|_{x=0} = 1, A_3|_{x=1} = 0, A_3|_{y=0} = A_3|_{y=1}$$

Global solution behaviour [1]

$$0 < \eta_m \ll 1 \Rightarrow$$

write formal asymptotic expansion in η_m:

$$A_3(x, y, t) = \sum_{j=0}^{\infty} a_{3,j}(x, y, t)\ \eta_m^j$$

Substitute expansion into PDE and check first-order term (setting $\eta_m = 0$); this gives hyperbolic PDE:

$$\frac{\partial a_{3,0}}{\partial t} = -\mathbf{v} \cdot \nabla a_{3,0}$$

initial solution stays constant on sub-characteristics given by:

$$(\dot{x}, \dot{y})^T = \mathbf{v}$$

Global solution behaviour [2]

As $\nabla \cdot \mathbf{v} = 0$, the only *critical points* in ODE system are center points or saddle points ($\rightsquigarrow$ *'field amplification'*).

At some point of time, the solution $a_{3,0}(x, y, t)$ can not satisfy the boundary conditions of the original PDE model: *boundary (and internal) layers* are formed of width $\mathcal{O}(\sqrt{\eta_m})$ ($\rightsquigarrow$ *'magnetic flux concentrates at edges of convective cells'*).

For $t \to \infty$ the solution reaches a *non-trivial steady-state*, in which the diffusion and convection terms settle down to an *equilibrium*.

Global solution behaviour [3]

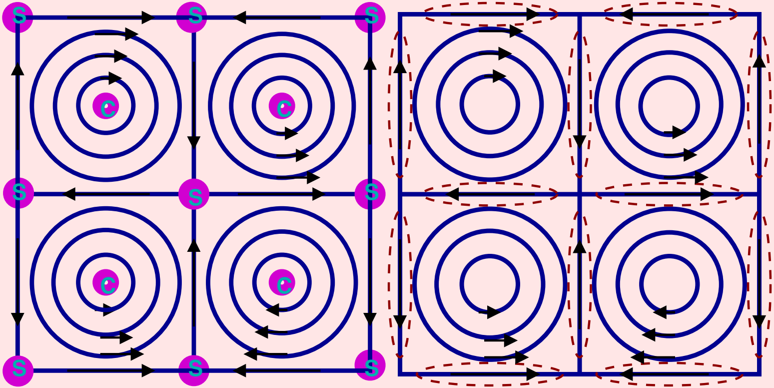

The numerical algorithm for the 2D case

- advection-diffusion-reaction PDE(s)
- decoupling of physical and grid PDEs
- grid PDEs: system of heat eq's with artificial time
- fixed time steps Δt
- Implicit-explicit time integration: 1-SBDF
- 'freezing' of non-linear terms in PDEs
- BiCGstab + diagonal preconditioning

Transformation of the PDE model [1]

$$\frac{\partial A_3}{\partial t} = -v_1 \frac{\partial A_3}{\partial x} - v_2 \frac{\partial A_3}{\partial y} + \eta_m \Delta A_3$$

$$\xi = \xi(x, y, t), \quad \eta = \eta(x, y, t), \quad \theta = t$$

Using the chain rule of differentiation:

$$A_{3,t} = A_{3,\theta}\theta_t + A_{3,\xi}\xi_t + A_{3,\eta}\eta_t.$$

We can also find that

$$\xi_t = -x_\theta \xi_x - y_\theta \xi_y = -\frac{1}{\mathcal{J}}(x_\theta y_\eta - y_\theta x_\eta)$$

Recall:

$$\mathcal{J} = x_\xi y_\eta - x_\eta y_\xi$$

Transformation of the PDE model [2]

Using a similar relation for η_t gives us

$$A_{3,t} = A_{3,\theta} + \frac{A_{3,\xi}}{\mathcal{J}}(x_\eta y_\theta - x_\theta y_\eta) + \frac{A_{3,\eta}}{\mathcal{J}}(x_\theta y_\xi - x_\xi y_\theta).$$

Since $\xi_x = \frac{y_\eta}{\mathcal{J}}, \xi_y = -\frac{x_\eta}{\mathcal{J}}, \eta_y = \frac{x_\xi}{\mathcal{J}}$ and $\eta_x = -\frac{y_\xi}{\mathcal{J}}$, we find for the first-order spatial derivative terms:

$$A_{3,x} = \frac{1}{\mathcal{J}}(A_{3,\xi} y_\eta - A_{3,\eta} y_\xi)$$

and

$$A_{3,y} = \frac{1}{\mathcal{J}}(A_{3,\eta} x_\xi - A_{3,\xi} x_\eta).$$

Transformation of the PDE model [3]

PDE in computational coordinates becomes:

$$\mathcal{J} A_{3,\theta} + A_{3,\xi}(x_\eta y_\theta - x_\theta y_\eta) + A_{3,\eta}(x_\theta y_\xi - x_\xi y_\theta)$$

$$= A_{3,\xi}(-v_1 y_\eta + v_2 x_\eta) + A_{3,\eta}(v_1 y_\xi - v_2 x_\xi) +$$

$$\eta_m [(\frac{x_\eta^2 + y_\eta^2}{\mathcal{J}} A_{3,\xi})_\xi - (\frac{x_\xi x_\eta + y_\xi y_\eta}{\mathcal{J}} A_{3,\eta})_\xi -$$

$$(\frac{x_\xi x_\eta + y_\xi y_\eta}{\mathcal{J}} A_{3,\xi})_\eta + (\frac{x_\xi^2 + y_\xi^2}{\mathcal{J}} A_{3,\eta})_\eta]$$

$$\boxed{\mathcal{J} = x_\xi y_\eta - x_\eta y_\xi}$$

Numerical results; four-cell convection [1]

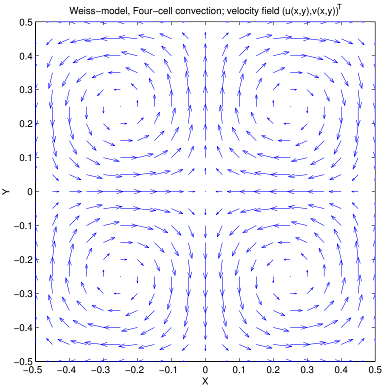

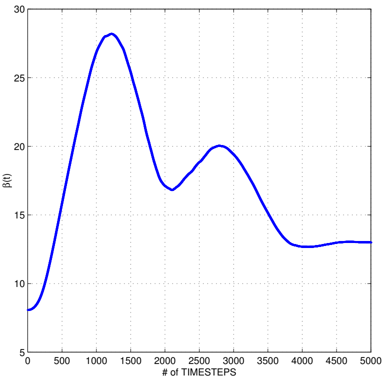

Numerical results; four-cell convection [2]

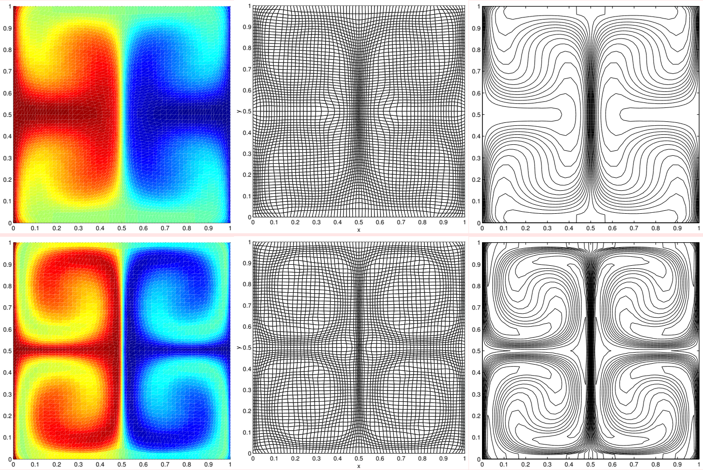

Numerical results; four-cell convection [3]

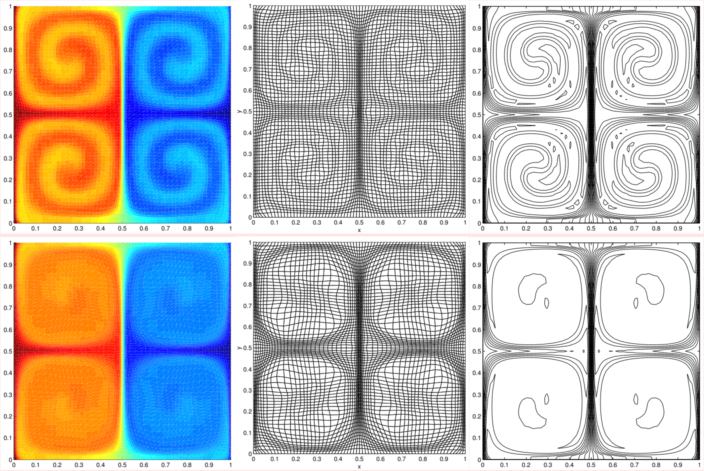

Application 3: the 2D Euler equations

$$\frac{\partial}{\partial t}\begin{pmatrix}\rho \\ \rho u \\ \rho v \\ E\end{pmatrix} + \frac{\partial}{\partial x}\begin{pmatrix}\rho u \\ \rho u^2 + p \\ \rho u v \\ u(E+p)\end{pmatrix} + \frac{\partial}{\partial y}\begin{pmatrix}\rho v \\ \rho u v \\ \rho v^2 + p \\ v(E+p)\end{pmatrix} = \begin{pmatrix}0 \\ 0 \\ 0 \\ 0\end{pmatrix}$$

ρ : density
$(\rho u, \rho v)^T$: momentum vector
E : total energy
p : pressure $= (\gamma - 1)(E - \rho\frac{u^2+v^2}{2})$
Write hyperbolic PDE system as:

$$\frac{\partial \mathcal{Q}}{\partial t} + \frac{\partial \mathcal{F}_1(\mathcal{Q})}{\partial x} + \frac{\partial \mathcal{F}_2(\mathcal{Q})}{\partial y} = \mathcal{G}(x, y, \mathcal{Q})$$

A typical non-uniform finite volume cell $A_{i+\frac{1}{2},j+\frac{1}{2}}$

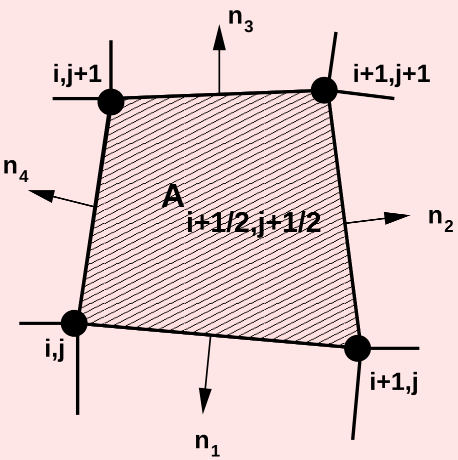

Discretization of the grid PDEs

⋆ Given a non-uniform partitioning $\{A_{i+\frac{1}{2},j+\frac{1}{2}}\}_{i,j}$ of Ω_p, where $A_{i+\frac{1}{2},j+\frac{1}{2}}$ is a quadrangle with four vertices $\mathbf{x}_{i+k,j+l}$, $0 \leq k, l \leq 1$ (denote numerical approximations to $\mathbf{x} = \mathbf{x}(\xi, \eta)$ by $\mathbf{x}_{i,j} = \mathbf{x}(\xi_i, \eta_j)$)

⋆ Subdivide $\Omega_c = \{(\xi, \eta) | \ 0 \leq \xi \leq 1, \ 0 \leq \eta \leq 1\}$ uniformly: $(\xi_i, \eta_j) | \ \xi_i = i\Delta\xi, \ \eta_j = j\Delta\eta; \ 0 \leq i \leq I_\xi + 1, \ 0 \leq j \leq I_\eta + 1$

⋆ Discretize the elliptic system of grid PDEs by second-order central finite differences

⋆ Apply a Gauß-Seidel iteration method to the resulting system of algebraic equations

A conservative solution-updating method

- Having computed the new grid, the solution values Q have to be updated on this grid by interpolation
(Tang et al '03 use a conservative interpolation method)
  - ⋆ Simple linear interpolation is not good enough
- Denote with $\mathbf{x}_{i,j}$ & $\tilde{\mathbf{x}}_{i,j}$ the coordinates of old and new grid points ($\mathbf{x}_{i,j}$ moves to $\tilde{\mathbf{x}}_{i,j}$ after Gauß-Seidel iterations)
- Using a perturbation technique and assuming small grid speeds, then the following mass-conservation is satisfied:

$$\boxed{\sum_{i,j} |\tilde{A}_{i+\frac{1}{2},j+\frac{1}{2}}| \; \tilde{\mathcal{Q}}_{i+\frac{1}{2},j+\frac{1}{2}} = \sum_{i,j} |A_{i+\frac{1}{2},j+\frac{1}{2}}| \; \mathcal{Q}_{i+\frac{1}{2},j+\frac{1}{2}}}$$

where $|A|$ is the area of cell A

Finite volume discretization on non-uniform grids [1]

$$\boxed{\frac{\partial \mathcal{Q}}{\partial t} + \frac{\partial \mathcal{F}_1(\mathcal{Q})}{\partial x} + \frac{\partial \mathcal{F}_2(\mathcal{Q})}{\partial y} = \mathcal{G}(x, y, \mathcal{Q})}$$

Integration over the finite control volume $A_{i+\frac{1}{2},j+\frac{1}{2}}$:

$$\boxed{\frac{\partial}{\partial t} \iint_{A_{i+\frac{1}{2},j+\frac{1}{2}}} \mathcal{Q}\ dxdy + \sum_{l=1}^{4} \int_{s_l} \mathbf{F}_{\mathbf{n}^l}(\mathcal{Q})|_{(x,y)\in s_l}\ ds = \iint_{A_{i+\frac{1}{2},j+\frac{1}{2}}} \mathcal{G}\ dxdy}$$

with $\mathbf{F}_{\mathbf{n}^l}(\mathcal{Q}) = \mathcal{F}_1 n_x^l + \mathcal{F}_2 n_y^l$ and $\mathbf{F}_{\mathbf{n}^l} = \mathbf{F}^+_{\mathbf{n}^l} + \mathbf{F}^-_{\mathbf{n}^l}$

Discretization $\Rightarrow$

Finite volume discretization on non-uniform grids [2]

$$\mathcal{Q}^{n+1}_{i+\frac{1}{2},j+\frac{1}{2}} = \mathcal{Q}^{n}_{i+\frac{1}{2},j+\frac{1}{2}} - \frac{\Delta t}{|A_{i+\frac{1}{2},j+\frac{1}{2}}|}\Big\{\mathcal{F}^{-}_{\mathbf{n}^1}(\mathcal{Q}^{n}_{i+\frac{1}{2},j-\frac{1}{2}}) + \mathcal{F}^{-}_{\mathbf{n}^2}(\mathcal{Q}^{n}_{i+\frac{3}{2},j+\frac{1}{2}})$$

$$+\mathcal{F}^{-}_{\mathbf{n}^3}(\mathcal{Q}^{n}_{i+\frac{1}{2},j+\frac{3}{2}}) + \mathcal{F}^{-}_{\mathbf{n}^4}(\mathcal{Q}^{n}_{i-\frac{1}{2},j+\frac{1}{2}}) + \sum_{l=1}^{4}\mathcal{F}^{+}_{\mathbf{n}^l}(\mathcal{Q}^{n}_{i+\frac{1}{2},j+\frac{1}{2}})\Big\} + \Delta t\,\mathcal{G}^{n}_{i+\frac{1}{2},j+\frac{1}{2}}$$

The time step size Δt is determined every time step by

$$\Delta t = \frac{\min(\Delta x, \Delta y)\ CFL}{\max|\lambda|},$$

where λ are the eigenvalues of the Jacobian matrix $\frac{\partial \mathbf{F}}{\partial \mathcal{Q}}$

Decoupling of the grids and physical PDEs

Step 1 Partition Ω_c uniformly; give initial partitioning of Ω_p; compute initial grid values by a cell average of control volume $A_{i+\frac{1}{2},j+\frac{1}{2}}$ based on initial data $\mathcal{Q}(x,y,0)$.
In a loop over the time steps, update grid and solution and evaluate the PDE:

Step 2a Move grid $\mathbf{x}_{i,j}$ to $\tilde{\mathbf{x}}_{i,j}$ by solving the discretized grid PDEs using Gauß-Seidel iterations.

Step 2b Compute $\tilde{\mathcal{Q}}_{i+\frac{1}{2},j+\frac{1}{2}}$ based on conservative interpolation. Repeat *step 2a* and *step 2b* for a fixed number of Gauß-Seidel iterations.

Step 3 Evaluate the physical PDEs by the finite volume method on the grid $\tilde{\mathbf{x}}_{i,j}$ to obtain $\mathcal{Q}^{n+1}_{i+\frac{1}{2},j+\frac{1}{2}}$ at t^{n+1}.

Step 4 Repeat *steps 2a, 2b* and *3* until $t = Tend$ is reached.

2D Riemann problem: shock waves

The first test example is a two-dimensional Riemann problem (config. 4 in Lax & Liu '98) and has the following initial data:

$$(\rho, u, v, p)_{t=0} = \begin{cases} (1.1, 0.0, 0.0, 1.1) & \text{if } x > 0.5, \; y > 0.5, \\ (0.5065, 0.8939, 0.0, 0.35) & \text{if } x < 0.5, \; y > 0.5, \\ (1.1, 0.8939, 0.8939, 1.1) & \text{if } x < 0.5, \; y < 0.5, \\ (0.5065, 0.0, 0.8939, 0.35) & \text{if } x > 0.5, \; y < 0.5. \end{cases}$$

They correspond to a left forward shock, right backward shock, upper backward shock and a lower forward shock, resp. The spatial domain Ω_p is $[0,1] \times [0,1]$ and $T_{end} = 0.25$.

Comparison: AL vs. BM-monitor vs. uniform grid

RUN #	*monitor*	α	*m*	*filter*	*runtime*
I	AL-monitor	0.01	-	on	0^h15^m
II	AL-monitor	0.1	-	on	0^h47^m
III	AL-monitor	2.0	-	on	2^h31^m
IV	AL-monitor	10.0	-	on	5^h48^m
V	AL-monitor	2.0	-	off	3^h04^m
VI	BM-monitor	-	2	off	$0h57^m$
VII	BM-monitor	-	1	off	1^h09^m
VIII	uniform (400 × 400)	-	-	-	1^h05^m
IX	uniform (600 × 600)	-	-	-	3^h50^m

Table: A shock wave model (configuration 4 from Lax & Liu '98)

Numerical results for the AL-monitor

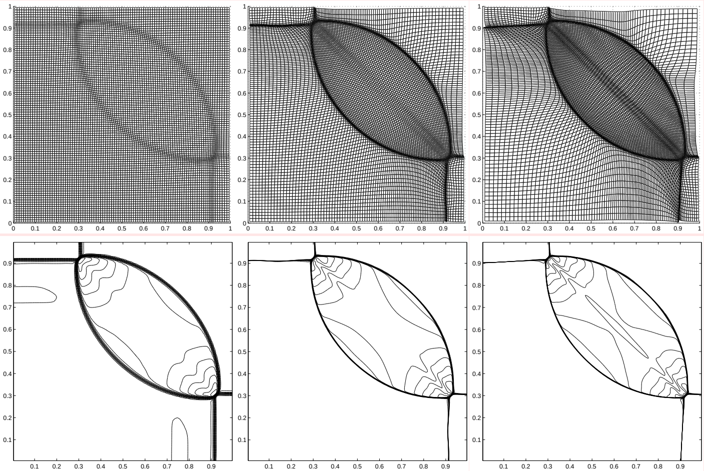

left: $\alpha = 0.01$, middle: $\alpha = 2$, right: $\alpha = 10$

Numerical results for the BM-monitor

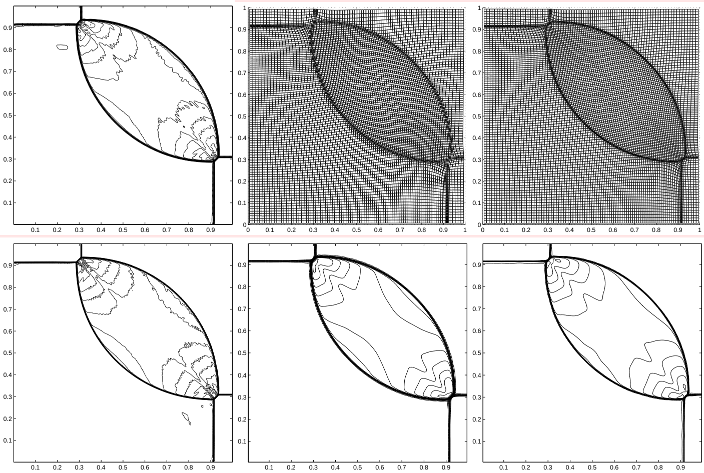

left: uniform grid 400^2 and 600^2, middle: $m = 2$, right: $m = 1$

The adaptive grid: a close-up near $(0.92, 0.15)$

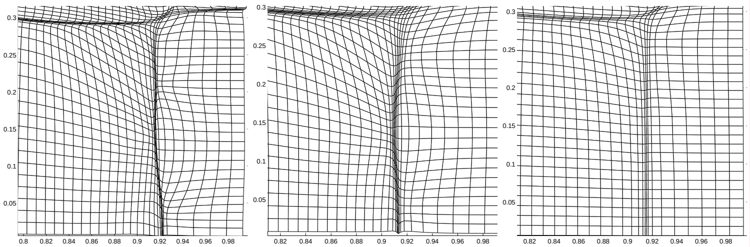

left: AL-monitor ($\alpha = 2$ & filter off); middle: AL-monitor ($\alpha = 2$ & filter on); right: BM-monitor with $m = 1$ (no filter needed)

The Rayleigh-Taylor instability model

⋆ This instability happens on an interface between fluids with different densities when an acceleration is directed from the heavy fluid to the light fluid

⋆ It has a fingering nature, with bubbles of light fluid rising into the ambient heavy fluid and spikes of heavy fluid falling into the light fluid

⋆ Here we have non-homogeneous BCs and an extra source term in the PDE-system: $\mathcal{G} = (0, 0, \rho g, \rho v g)^T$, where g is the acceleration due to gravity

Numerical results for Rayleigh-Taylor instability [1]

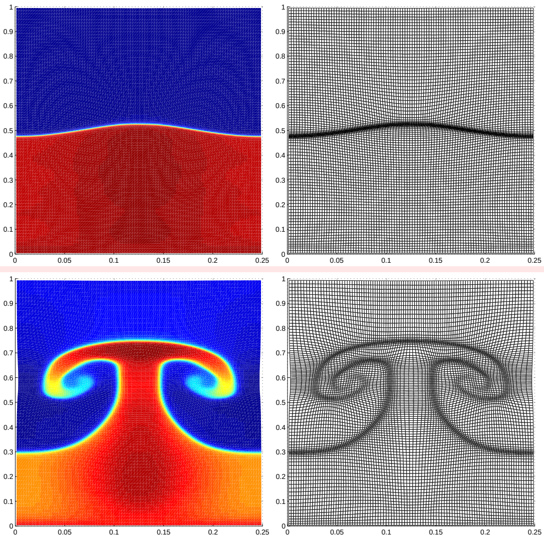

Results at $t = 0.5$, $t = 2.0$

Extension of Winslow to 3D

Minimization of grid-energy yields in 3D:

$$\begin{aligned}\nabla \cdot (\omega \nabla x) &= 0\\ \nabla \cdot (\omega \nabla y) &= 0\\ \nabla \cdot (\omega \nabla z) &= 0, \quad (x,y,z)^T \in [0,1]^3\end{aligned}$$

with

$$\omega = \alpha(t) + ||\nabla u||_2, \;\; \alpha(t) = \int\int\int_{\Omega_c} ||\nabla u||_2 \; d\xi d\eta d\zeta$$

Non-singular transformation? Theory?

Extension of Winslow to 3D

Minimization of grid-energy yields in 3D:

$$\nabla \cdot (\omega \nabla x) = \frac{\partial x}{\partial \tau}$$
$$\nabla \cdot (\omega \nabla y) = \frac{\partial y}{\partial \tau}$$
$$\nabla \cdot (\omega \nabla z) = \frac{\partial z}{\partial \tau}, \quad (x, y, z)^T \in [0,1]^3$$

with

$$\omega = \alpha(t) + ||\nabla u||_2, \ \alpha(t) = \int\int\int_{\Omega_c} ||\nabla u||_2 \ d\xi d\eta d\zeta$$

Non-singular transformation? Theory?

Transformation of ‘a blow-up PDE’

The PDE $\frac{\partial u}{\partial t} = \Delta u + u^p$

transforms via $(x, y, z, t) \rightarrow (\xi, \eta, \zeta, \theta)$; with $t = \theta$ to:

$$u_\theta + \frac{1}{\mathcal{J}}[u_\xi(-x_\theta(y_\eta z_\zeta - y_\zeta z_\eta) - y_\theta(x_\zeta z_\eta - x_\eta z_\zeta) - z_\theta(x_\eta y_\zeta - x_\zeta y_\eta)) + u_\eta(-x_\theta(y_\zeta z_\xi - y_\xi z_\zeta)$$

$$-y_\theta(x_\xi z_\zeta - x_\zeta z_\xi) - z_\theta(x_\zeta y_\xi - x_\xi y_\zeta)) + u_\zeta(-x_\theta(y_\xi z_\eta - y_\eta z_\xi) - y_\theta(x_\eta z_\xi - x_\xi z_\eta) - z_\theta(x_\xi y_\eta - x_\eta y_\xi))] =$$

$$\frac{1}{\mathcal{J}}[\left(\frac{(y_\eta z_\zeta - y_\zeta z_\eta)^2 + (x_\zeta z_\eta - x_\eta z_\zeta)^2 + (x_\eta y_\zeta - x_\zeta y_\eta)^2}{\mathcal{J}} u_\xi\right)_\xi +$$

$$\left(\frac{(y_\eta z_\zeta - y_\zeta z_\eta)(y_\zeta z_\xi - y_\xi z_\zeta) + (x_\zeta z_\eta - x_\eta z_\zeta)(x_\xi z_\zeta - x_\zeta z_\xi) + (x_\eta y_\zeta - x_\zeta y_\eta)(x_\zeta y_\xi - x_\xi y_\zeta)}{\mathcal{J}} u_\eta\right)_\xi +$$

$$\left(\frac{(y_\eta z_\zeta - y_\zeta z_\eta)(y_\xi z_\eta - y_\eta z_\xi) + (x_\zeta z_\eta - x_\eta z_\zeta)(x_\eta z_\xi - x_\xi z_\eta) + (x_\eta y_\zeta - x_\zeta y_\eta)(x_\xi y_\eta - x_\eta y_\xi)}{\mathcal{J}} u_\zeta\right)_\xi +$$

$$\left(\frac{(y_\zeta z_\xi - y_\xi z_\zeta)(y_\eta z_\zeta - y_\zeta z_\eta) + (x_\xi z_\zeta - x_\zeta z_\xi)(x_\zeta z_\eta - x_\eta z_\zeta) + (x_\zeta y_\xi - x_\xi y_\zeta)(x_\eta y_\zeta - x_\zeta y_\eta)}{\mathcal{J}} u_\xi\right)_\eta + \ldots\ldots$$

with $\mathcal{J} = z_\zeta(x_\xi y_\eta - x_\eta y_\xi) - z_\eta(x_\xi y_\zeta - x_\zeta y_\xi) + z_\xi(x_\eta y_\zeta - x_\zeta y_\eta)$

Blow-up models (intro) [1]

Application areas:

- Combustion models & chemical reaction dynamics
- Population dynamics: motion of colonies of micro-organisms
- Plasma physics: wave motion in fluids and electromagnetic fields

Blow-up models (intro) [2]

Consider the ODE:

$$\begin{cases} \dot{u} = u^p, \; p > 1 \\ u(0) = u_0 \end{cases}$$

Exact solution:

$$u(t) = \frac{1}{[(p-1)(T-t)]^{p-1}}, \quad T = \frac{1}{u_0^{p-1}(p-1)}$$

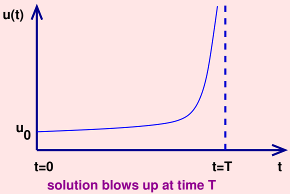

Blow-up models (intro) [3]

Consider the PDE:

$$\begin{cases} \frac{\partial u}{\partial t} = \Delta u + u^p, \; p > 1 \\ u|_{\partial\Omega} = 0, u(x,0) = u_0(x) \end{cases}$$

Kaplan 1963: if u_0 smooth and large enough, then the solution u is regular for every $0 \leq t < T$, but

$$\lim_{t \to T} ||u(\cdot, t)||_{\mathcal{L}^\infty} = +\infty$$

Blow-up models (intro) [4]

Another PDE example:

$$\begin{cases} \frac{\partial u}{\partial t} = \frac{\partial^2 u}{\partial x^2} - u + u^p, \ x \in (0,\pi), \ t > 0 \\ u(x,0) = u_0(x) \geq 0, \ x \in (0,\pi), \\ u(0,t) = u(\pi,t) = 0, \ t > 0 \end{cases}$$

- Let $f = \int_0^\pi u(x,t)\sin(x)\,dx$, then $\dot{f} = \int_0^\pi (\frac{\partial^2 u}{\partial x^2} - u^p)\sin(x)\,dx - f$
  Via Hölder's inequality: $\dot{f} \geq -2f + \frac{f^p}{2^{p-1}}$
- If $f(0) > 2^{\frac{p}{p-1}}$, then $f(t) \to \infty$ in finite time
  By Cauchy-Schwartz: $f \leq ||u||_{\mathcal{L}^2(0,\pi)} \, ||\sin(x)||_{\mathcal{L}^2(0,\pi)}$
- Thus $f \to \infty$ implies $||u||_{\mathcal{L}^2(0,\pi)} \to \infty$
  $\Rightarrow$ u leaves $\mathcal{L}^2(0,\pi)$ in finite time

Adaptive time steps with a Sundman transformation [1]

Explicit Euler with fixed Δt for $\begin{cases} \dot{u} = u^p \\ u(0) = 1 \end{cases}$:

$$u^{n+1} = u^n + \Delta t \, (u^n)^p \quad \Rightarrow$$

Numerical solution exists *for all* $t^n = n\Delta t$ (i.e. no blow up...)

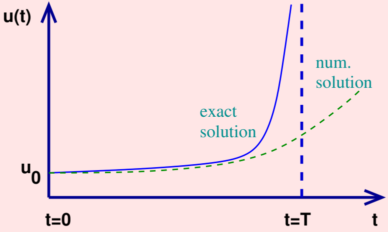

Adaptive time steps with a Sundman transformation [2]

Explicit Euler + central FD's for $u_t = u_{xx} + u^p$:

$$\frac{u_j^{n+1} - u_j^n}{\Delta t^n} = \frac{u_{j+1}^n - 2u_j^n + u_{j-1}^n}{(\Delta x)^2} + (u_j^n)^p$$

with $\Delta t^n = \frac{\Delta\theta}{||u^n||_\infty^{p-1}}$ and constant $\Delta\theta$

($\sim$ a Sundman *time* transformation $t(\theta) = \frac{\theta}{||u||_\infty^{p-1}}$)

$\Rightarrow$ for sufficiently small Δx (+ stab. restriction on Δt^n), the numerical solution blows up at $T_{\Delta x}$ and $\lim_{\Delta x \to 0} T_{\Delta x} = T$ (Abia et al, 2001)

Adaptive time steps with a Sundman transformation [3]

In terms of scaling invariance and self-similarity:

Consider the ODE $\dot{u} = u^2$, i.e. $p = 2$, then using a fictive computational time variable θ gives rise to a new ODE system with

$$\left\{ \begin{array}{l} \frac{du}{d\theta} = u \\ \frac{dt}{d\theta} = \frac{1}{u} \end{array} \right.$$

that is *invariant* under the scaling $t \to \lambda t, \; u \to \lambda^{-1} u$ and for which the numerical solution u^n uniformly approximates the true *self-similar* solution $u(t) = -\frac{1}{t}$ of the original ODE for $\Delta\theta \to 0$. (Budd, Piggott, Leimkuhler et al)

The numerical algorithm in 3D

- decoupling of blow-up and grid PDEs
- grid PDEs: system of heat equations with artificial time

- central finite differences on non-uniform grid for Δ
- 'freezing' of non-linear terms in PDEs in each time step

- implicit Euler for Δ and explicit for reaction term
- BiCGstab + ILU-preconditioning for underlying linear systems

- variable Δt using Sundman-transformation

Blow-up in 3D [1]

Case 1:

$$u(x,y,z,0) = \exp(-30((x-\tfrac{1}{2})^2 + (y-\tfrac{1}{2})^2 + (z-\tfrac{1}{2})^2)$$
$$(p = \tfrac{3}{2},\quad 11^3/21^3/41^3 \text{ grid; with or without Sundman } t(\theta))$$

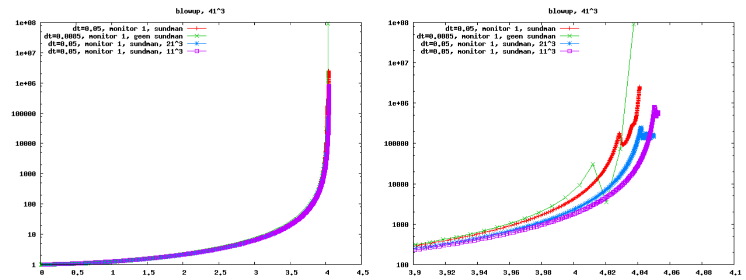

Maximum value of u as a function of time t.

Blow-up in 3D [2]

Case 1 (cntd.):

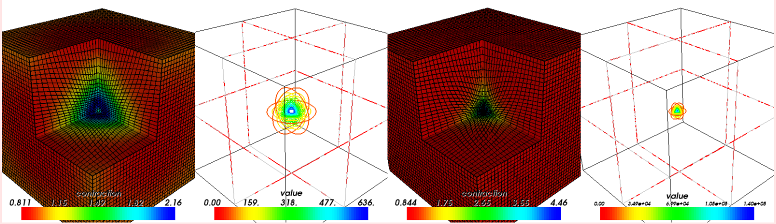

Adaptive grids and numerical solutions at two points of time just before blow-up (note the scale of the solution in each of the plots)

Blow-up in 3D [3]

Case 2:

$u(x, y, z, 0) = 10 \sin(\pi x) \sin(\pi y) \sin(\pi z)$
$(p = 3, \quad 11^3/21^3/41^3$ grid; with or without Sundman $t(\theta))$

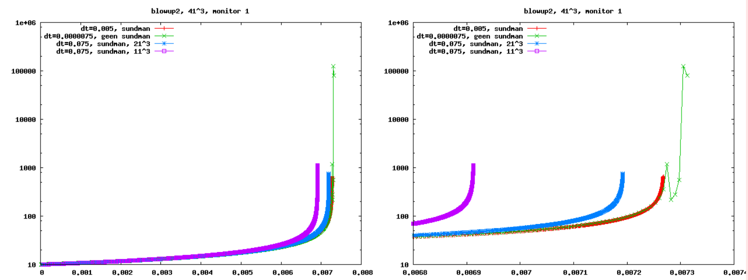

Maximum value of u as a function of time t. (blow-up time in our experiments $\sim$ T from Liang & Lin, 2005: ≈ 0.007249)

Blow-up in 3D [4]

Case 2 (cntd.):

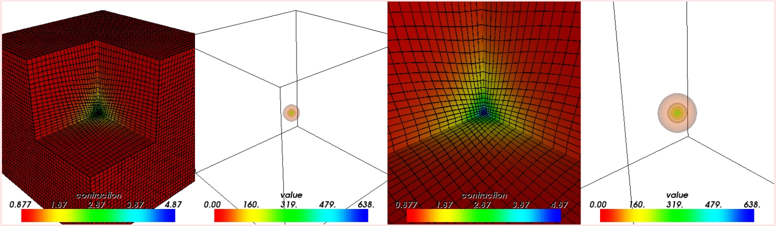

Adaptive grid and numerical solution just before blow-up
(right plot: close-up of grid and solution)

Summary of Part 1-4

- 1D adaptive moving grids: a lot of theory is available with many applications!!

- 2D on "simple" domains: some theory, but several applications!

- the 3D case: theory is difficult and only a few applications yet: in development.

Final remarks

• ALL adaptive moving grid methods (r-refinement), when restricted to 1 space dimension, are related to:

⋆ either: method of characteristics (velocity based grids)

⋆ or: equidistribution principle (location based grids)

⋆ or: a combination of the above two!